

## Supramolecular Chirality Measurement of an Optically Anomalous Single Crystal

Takunori Harada,\*<sup>1</sup> Natsuyo Asano,<sup>2</sup> Nobuo Tajima,<sup>3</sup> and Hiroshi Moriyama<sup>1</sup>

<sup>1</sup>Department of Chemistry, Faculty of Science, Toho University, 2-2-1 Miyama, Funabashi, Chiba 274-8510

<sup>2</sup>Shimadzu Corporation, 1 Nishinokyo-Kuwabaracho, Nakagyo-ku, Kyoto 604-8511

<sup>3</sup>First-Principles Simulation Group, Computational Materials Science Center, National Institute for Materials Science (NIMS), 1-2-1 Sengen, Tsukuba, Ibaraki 305-004

(Received January 6, 2012; CL-120010; E-mail: takunori.harada@sci.toho-u.ac.jp)

The compound 1,8-dihydroxyanthraquinone (DHA) forms chiral crystals composed of several distinct homogeneous regions giving triclinic symmetry in an apparently tetragonal unit cell. True chirality measurement of an optically anomalous DHA crystal was achieved for the first time using a universal chiroptical spectrophotometer in the UV–vis wavelength range.

Until now, universal chiroptical spectrophotometer (UCS) systems<sup>1–3</sup> based on the Stokes–Mueller matrix approach<sup>1,4</sup> (such as UCS-1:<sup>1</sup> JASCO J-800KCM, a vertical-type dual-purpose circular dichroism (CD) and diffuse reflectance CD (DRCD) instrument; UCS-2:<sup>2</sup> JASCO J-800KCMF; and UCS-3:<sup>3</sup> JASCO J-800KCMFII) have been constructed for use in the development of solid-state chiral chemistry. They are capable of separately measuring all polarization phenomena (CD, linear dichroism (LD), linear birefringence (LB), and circular birefringence (CB) or optical rotatory dispersion) and abstracting the true polarization phenomena out of mixed signals in the solid state. Physicochemical knowledge of solid samples, e.g., single crystals,<sup>1,5</sup> films,<sup>6</sup> microcrystalline crystals,<sup>2,3,7</sup> etc., is easily obtainable using UCS systems. However, solid-state chirality measurements for single crystals require great care, taking into account their spectroscopic nature, optical symmetry, etc. Generally, the true chirality measurement of an optically transparent single crystal belongs to a uniaxial crystal with higher symmetry than an optically biaxial crystal, e.g., orthorhombic, monoclinic, and triclinic systems, can be directly measured using a UCS system when the LB values of the sample are smaller than 30°. However, there are exceptional cases even among uniaxial crystals with small LB values because crystal systems with enantiomorphous twinning or sector twins<sup>8</sup> result in decreased symmetry. An optically inhomogeneous crystal comprising discrete sectors and domains represents an optically anomalous crystal in which the optical symmetry is lower than the apparent structural symmetry.<sup>9</sup> In this case, true chirality measurement is impossible because of the difficulty of eliminating the contribution of macroscopic anisotropies to the chirality signal observed in an optically inhomogeneous sample, even using a UCS system dedicated to solid samples. This is because the UCS system was constructed on the basic assumption that the samples are optically homogeneous. Thus, single crystals with larger LB values (>30°) or optically inhomogeneous crystals must be adapted to the diffuse reflectance method<sup>10</sup> or the matrix method, i.e., the KBr disc and nujol mull, in which they are regarded as optically quasi-isotropic. Therefore, it is necessary that we cautiously select the most suitable method by measuring the absolute LB value and/or checking the optical

homogeneity using an optically sensitive polarizing microscope by the optical null method.

In this paper, to demonstrate true CD measurement of an optically anomalous crystal, we chose crystalline 1,8-dihydroxyanthraquinone (DHA) with polymorphic variability as a first sample. We report for the first time the true supramolecular chirality measurement of optically anomalous crystals having several distinct homogeneous sectors in the UV–vis wavelength range. The molecular structure of DHA is shown in Figure 1a, together with the electric dipole transition moment indicated for the lowest energy  $\pi$ – $\pi^*$  transition.<sup>11</sup> The crystal structure of DHA was determined previously and belongs to the  $P4_1(3)$  space group.<sup>11,12</sup> Thus, DHA exhibits optical activity only in the crystalline state because of the chiral supramolecular arrangement of the nonchiral molecule. Despite the evidently tetragonal morphology, the crystals seem to show noticeable LB even if viewed along the optical axis, i.e., the [001] direction, and complex birefringence patterns. This is because the DHA crystal has several distinct homogeneous regions that classify it as an optically anomalous crystal.<sup>13</sup> The optical symmetry for an optically anomalous crystal possessing symmetrically organized sectors is lower than the apparent structural symmetry (which is tetragonal) so that an individual sector shows higher symmetry than the composite crystal (triclinic). The higher symmetry of the crystal sector is determined as usual by X-ray diffraction, and the lower symmetry of the composite is observed using a polarizing microscope. Therefore, special regard should be paid to larger intrinsic LB and crystal homogeneity when performing chirality measurements. A DHA single-crystal plate belonging to the  $P4_1(3)$  space group was recrystallized from acetone/acetonitrile (50:50 (v:v)) solution in 1–2 days (Figure 1a). From an isogyre of the conoscopic observation, it was confirmed that DHA single crystals were categorized as biaxial, not uniaxial,<sup>14</sup> and formed systematic sectors separated by the (110) diagonal boundaries that had either positive or negative optical anisotropy as shown in Figure 1a. A thin plate of DHA (<20  $\mu\text{m}$ ) was composed simply of four sectors divided by diagonal lines, although complex domains with characteristic heterochiral pinwheels<sup>11</sup> appeared over the 40  $\mu\text{m}$  thickness.

We tried to measure the artifact-free CD and electronic absorption spectra of a DHA single crystal (<20  $\mu\text{m}$ ) across the whole UV–vis wavelength range of the UCS system (UCS-4).<sup>15</sup> The solid-state electronic absorption spectrum of a KBr disc of DHA crystal diluted within a KBr matrix is shown in Figure 1b, together with one in acetonitrile solution for comparison.

It was confirmed from the powder X-ray diffraction pattern that the DHA crystal structure does not change in the process of disc formation (Figure S1).<sup>15</sup> The peak positions of the

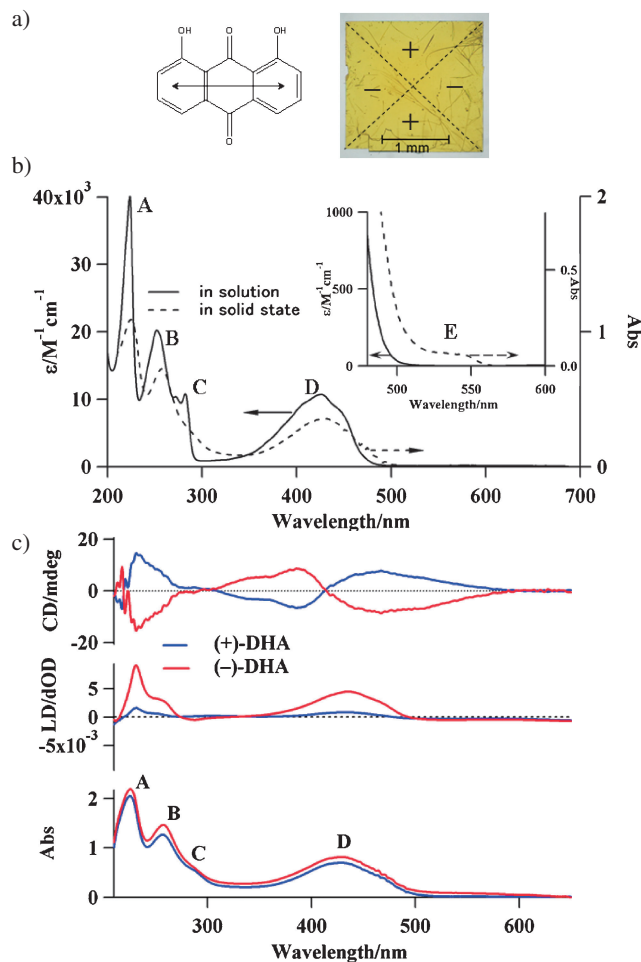


**Figure 1.** (a) 1,8-Dihydroxyanthraquinone (DHA) crystal (1.9 mm × 2.0 mm × 20 μm) in white light viewed along [001]. The molecular structure of DHA is shown together with the electric dipole transition moment indicated for the lowest  $\pi$ - $\pi^*$  transition. (b) Electronic absorption spectra of DHA in acetonitrile solution and the solid state (KBr disc and single crystal (20 μm thickness (inset))) are shown. (c) The solid-state CD, LD, and electronic absorption spectra of KBr discs measured using UCS-4 for the (+)- and (-)-DHA enantiomeric crystals (diluted within KBr matrix: 0.016 (blue line) and 0.016 wt % (red line)).

transitions denoted A–E in high-energy order are almost identical to those in the solution state, except for the E transition. Transitions A–D and E belong to allowed  $\pi$ - $\pi^*$  and forbidden  $n$ - $\pi^*$  transitions, respectively. The low-energy transition E is only observed in the single crystal and neither in the KBr disc nor acetonitrile solution because the absorption coefficient of the forbidden E transition is very small compared with other allowed transitions and it is impossible to make a transparent KBr disc with a high concentration (>0.16 wt %) in which the D transition signal is saturated (Figure S2).<sup>15</sup> The reason for observing a low-energy shoulder at ca. 530 nm (E transition) that was not present in the polar solution is discussed below.

Solid-state CD spectra of enantiomorphous DHA crystals in the UV–vis wavelength range, together with LD and absorption

spectra, are shown in Figure 1c. Mirror image CD spectra could be obtained in individual sectors cut from enantiomorphous single crystals. The observed CD spectra were checked for correctness using Stokes–Mueller matrix analysis. The 50 kHz signal detected by UCS-4 can be expressed as follows:

$$\begin{aligned} \text{Signal}_{50\text{kHz}} &= G_1 \{ (P_x^2 + P_y^2) [\text{CD} + 1/2(\text{LD}'\text{LB} - \text{LB}'\text{LD}) \\ &+ (\text{LD}' \sin 2\theta - \text{LD} \cos 2\theta) \sin \alpha] \} \\ &+ G_1 \{ (P_x^2 - P_y^2) \sin 2a [(\text{LB}' \sin 2\theta - \text{LB} \cos 2\theta) \\ &+ [-\text{CB} + 1/2(\text{LD}^2 + \text{LB}^2 - \text{LD}'^2 - \text{LB}'^2) \sin 4\theta \\ &+ (\text{LD}'\text{LD} + \text{LB}'\text{LB}) \cos 4\theta] \sin \alpha \} \end{aligned} \quad (1)$$

$G_1$  is the apparatus constant related to the sensitivity of the spectrometer at 50 kHz.  $\text{LD}'$  and  $\text{LB}'$  are 45° preference LD and LB, respectively.  $P_x^2$  and  $P_y^2$  are the transmittance of the photomultiplier along the  $x$  and  $y$  directions, and  $a$  is the azimuth angle of its optical axis with respect to the  $x$  axis.  $\theta$  is the rotation angle of the sample, and  $\alpha$  is the residual static birefringence of the photoelastic modulator (PEM). The solid-state CD spectra were checked for the effect of artifact signals arising from the interaction between the macroscopic anisotropies of the sample and the nonideal characteristics of the polarization–modulation instrument.<sup>1</sup> The artifact signals have terms that are both dependent and independent of sample rotation in the plane perpendicular to the light beam, as shown in eq 1.<sup>1</sup> The residual birefringence,  $\alpha$ , of our carefully selected PEM has a value of  $-0.16^\circ$  at 400 nm, hence  $\sin \alpha$  is  $-2.8 \times 10^{-3}$  OD. Thus, the terms multiplied by  $\sin \alpha$  must be negligibly small. Shindo reported<sup>16</sup> that the value of the polarization characteristics of the detector,  $P$ ,<sup>17</sup> is of the order of  $10^{-4}$  at 450 nm for a head-on type photomultiplier (Hamamatsu R-374). The terms multiplied by  $P$  were estimated to be of the order of  $10^{-7}$  at 350 nm as the LB values of the KBr discs were found to be of the order of  $10^{-3}$  OD. Solid-state CD signals hardly changed with sample rotation (data not shown), hence the angular-dependent terms multiplied by  $P$  are negligible. LD signals of current samples were measured to be of the order of  $10^{-3}$ – $10^{-4}$  OD (Figure 1c), hence the angular-independent terms,  $1/2(\text{LD}'\text{LB} - \text{LD}\text{LB}')$ , are  $10^1$ – $10^2$  times smaller than the true CD signal. Those parasitic terms can be removed from the detected 50 kHz signal using the analytical method.<sup>1</sup> Moreover, the absolute values of the dissymmetry factor,  $g_{\text{abs}}(\lambda)$ , i.e., the ratio  $\Delta A/A$  at a specific wavelength, for enantiomers are in fair agreement with each other ( $|g_{\text{abs}}| = 0.00045$  at 390 nm). Thus, we can conclude that the obtained CD spectra of KBr discs are artifact-free CD signal, i.e., pure CD signal, and the cut sector from a single crystal is enantiopure.

Similarly, the observed electronic absorption spectra of the DHA crystal were checked against theoretically simulated electronic absorption curves that were calculated from semi-empirical molecular orbital theory (ZINDO method<sup>18</sup>) using the Gaussian 03 program.<sup>19</sup> The ZINDO calculation was carried out for a molecular cluster (four molecules) that was selected from the X-ray crystal structure to contain the nearest molecule pairs in the crystal (Figure 2a).<sup>12</sup> Figure 2b shows the theoretically calculated absorption spectrum for the four-molecule cluster, together with the calculated spectrum for an isolated DHA molecule for comparison. The two spectra suggest that the solid-state spectrum of DHA is essentially a spectrum of this molecule

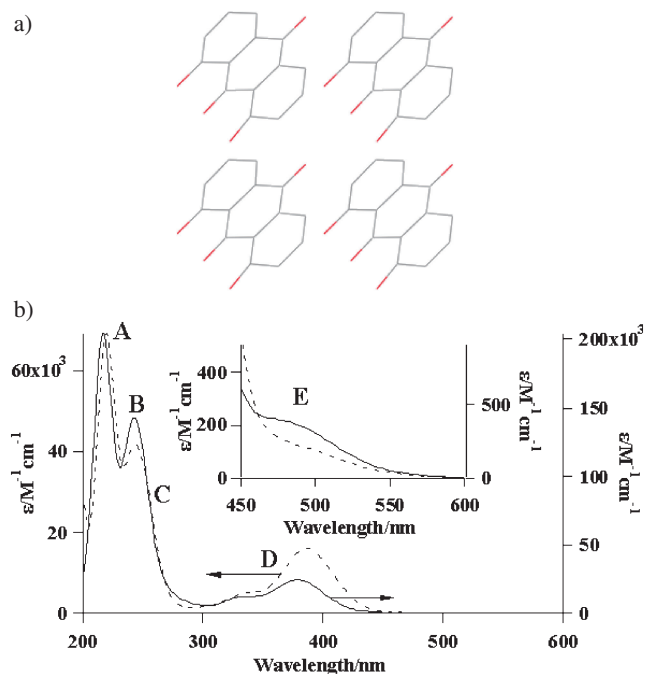


**Figure 2.** (a) Cluster of four DHA molecules, [DHA4], used for the ZINDO calculation. H atoms are omitted for clarity. (b) Calculated electronic absorption spectrum for the free component molecule and cluster: solid line, cluster; dotted line, single molecule.

without solvent effects. In the plotted wavelength range, the molecular cluster has four absorption bands (three  $\pi$ - $\pi^*$  states (A, B, and D) and one  $n$ - $\pi^*$  state (E)).

The peak positions generally agree well with those of the experimental electronic absorption curves measured using UCS-4 (except that the C transition is underneath B in the theoretically calculated spectra). The peak positions of the E and D bands may seem slightly different from those of the observed ones. Difference of this degree is very likely, however, because a trivial error in energy calculation affects the absorption curves in the longer wavelength region rather significantly. The low-energy E band is present in the calculated spectrum and in the experimentally observed spectrum of single crystal but not in the observed solution spectrum (Figure 1b). This band might be underneath the D band in acetonitrile solution because the  $n$ - $\pi^*$  transition tends to blue-shift in polar solution. However, in nonpolar solution, E transition with the molar extinction coefficient,  $15 \text{ M}^{-1} \text{ cm}^{-1}$ , which is ca. 600 times smaller than that of the D transition, is observed around 525 nm due to the bathochromic effect on the  $n$ - $\pi^*$  transition (Figure S3).<sup>15</sup> Judging from the results of the theoretical approach based on semiempirical molecular orbital theory and the Stokes–Mueller matrix analysis, we conclude that the solid-state CD spectra of DHA are reliable across the whole wavelength range and arise only from supramolecular chirality.

Single-crystal CD and electronic absorption measurements in the visible wavelength region (400–600 nm) have already been reported by Claborn et al. using a CD imaging microscope (CDIM) that was constructed to avoid linear biases that are common with electronic circular polarization modulation.<sup>11</sup>

There is a close resemblance between the reported CD spectra<sup>11</sup> and the single-crystal solid-state CD spectrum (Figure S4)<sup>15</sup> exhibiting spectral edges at 480 and 575 nm around low-energy transitions. They concluded that the CD signal was only associated with the  $n$ - $\pi^*$  transition. However, in our case, the CD signal detected by an R-374 photomultiplier tube (PMT) having a gain range of 80 dB<sup>20</sup> was saturated for the  $\pi$ - $\pi^*$  transitions as well as the electronic absorption signals and were not true signals. Thus, under conditions in which the E transition could be detected, the high-energy transitions could not also be detected by a CDIM equipped with a Cohu 4910 CCD detector having a gain range of 56 dB<sup>21</sup> that is narrower than that of the PMT.

In summary, by carefully selecting a method to suit an optically inhomogeneous sample containing several distinct homogeneous sectors that results in a decrease in symmetry relative to the apparent structural symmetry, we could measure the true CD spectra of the optically anomalous DHA crystal in the UV–vis wavelength region for the first time.

The authors thank R. Kuroda, Professor of the University of Tokyo, for helpful discussions.

#### References and Notes

- R. Kuroda, T. Harada, Y. Shindo, *Rev. Sci. Instrum.* **2001**, *72*, 3802.
- T. Harada, H. Hayakawa, R. Kuroda, *Rev. Sci. Instrum.* **2008**, *79*, 073103.
- T. Harada, Y. Miyoshi, R. Kuroda, *Rev. Sci. Instrum.* **2009**, *80*, 046101.
- a) T. Harada, T. Sato, R. Kuroda, *Chem. Phys. Lett.* **2005**, *413*, 445. b) T. Harada, T. Sato, R. Kuroda, *Chem. Phys. Lett.* **2008**, *456*, 268.
- a) T. Harada, Y. Shindo, R. Kuroda, *Chem. Phys. Lett.* **2002**, *360*, 217. b) T. Harada, R. Kuroda, H. Moriyama, *Chem. Phys. Lett.* **2012**, *530*, 126.
- a) Y. Shindo, K. Kani, J. Horinaka, R. Kuroda, T. Harada, *J. Plast. Film Sheeting* **2001**, *17*, 164. b) T. Harada, R. Kuroda, *Chem. Lett.* **2002**, 326. c) T. Harada, R. Kuroda, *Biopolymers* **2011**, *95*, 127.
- N. Asano, T. Harada, T. Sato, N. Tajima, R. Kuroda, *Chem. Commun.* **2009**, 899.
- A. V. Jagannadham, *Z. Kristallogr.* **1957**, *108*, 457.
- A. Prakash, *Z. Kristallogr.* **1965**, *122*, 272.
- I. Bilotti, P. Biscarini, E. Castiglioni, F. Ferranti, R. Kuroda, *Chirality* **2002**, *14*, 750.
- K. Claborn, E. Puklin–Faucher, M. Kurimoto, W. Kaminsky, B. Kahr, *J. Am. Chem. Soc.* **2003**, *125*, 14825.
- S. M. Zain, S. W. Ng, *Acta Crystallogr., Sect. E: Struct. Rep. Online* **2005**, *61*, o2921.
- B. Kahr, J. M. McBride, *Angew. Chem., Int. Ed. Engl.* **1992**, *31*, 1.
- M. Akizuki, *Nihon Kessho Gakkaishi* **2000**, *42*, 401.
- Supporting Information is available electronically on the CSJ–Journal Web site, <http://www.csj.jp/journals/chem-lett/index.html>.
- Y. Shindo, M. Nakagawa, *Rev. Sci. Instrum.* **1985**, *56*, 32.
- The polarization characteristic,  $P$ , of the detector is expressed as  $(P_x^2 - P_y^2) \sin 2a$ .
- a) J. Ridley, M. Zerner, *Theor. Chim. Acta* **1973**, *32*, 111. b) J. E. Ridley, M. C. Zerner, *Theor. Chim. Acta* **1976**, *42*, 223. c) M. C. Zerner, G. H. Loew, R. F. Kirchner, U. T. Mueller–Westerhoff, *J. Am. Chem. Soc.* **1980**, *102*, 589.
- M. J. Frisch, et al., *Gaussian 03 (Revision C.02)*, Gaussian, Inc., Wallingford CT, **2004**.
- Hamamatsu photonics K.K. Technical Note, Japan, **1999**.
- Cohu, Inc., Technical Note, San Diego, CA, USA.